Journal of the Neurological Sciences 399 (2019) 69–75

Contents lists available at ScienceDirect

Journal of the Neurological Sciences

journal homepage: www.elsevier.com/locate/jns

Clinical short communication

Clinical and neuroimaging features of the m.10197G > A mtDNA mutation: New case reports and expansion of the phenotype variability

Tolomeo D.[a,1], Rubegni A.[b,1], Severino M.[c], Pochiero F.[d], Bruno C.[e], Cassandrini D.[b], Madeo A.[f], Doccini S.[b], Pedemonte M.[e], Rossi A.[c], D'Amore F.[b], Donati M.A.[d], Di Rocco M.[f], Santorelli F.M.[b,*], Nesti C.[b,1]

[a] Department of Clinical and Experimental Medicine, University of Pisa, viale del Tirreno 331, 56128 Calambrone, Pisa, Italy
[b] IRCCS Fondazione Stella Maris, viale del Tirreno 331, 56128 Calambrone, Pisa, Italy
[c] Neuroradiology Unit, Istituto Giannina Gaslini, Largo G. Gaslini 5, 16147 Genova, Italy
[d] AOU Meyer Children Hospital, viale G. Pieraccini 24, 50139 Firenze, Italy
[e] Center of Translational and Experimental Myology, Istituto Giannina Gaslini, Largo G. Gaslini 5, 16147 Genova, Italy
[f] Unit of Rare Diseases, Istituto Giannina Gaslini, Largo G. Gaslini 5, 16147 Genova, Italy

ARTICLE INFO

Keywords:
Leigh syndrome
Complex I deficiency
ND3 gene
mtDNA

ABSTRACT

Complex I (CI) is the largest component of the mitochondrial respiratory chain (MRC) and it is made up of 7 mitochondrial DNA (mtDNA)-encoded and at least 38 nuclear DNA-encoded subunits. Isolated CI deficiency is the most common single enzyme deficiency in the heterogeneous group of MRC disorders and it is a relatively common etiology of Leigh-like syndrome (LS).

With a few exceptions, descriptions of the clinical spectrum of specific mutations in CI are scarce. We here present three unrelated Italian children who harbored the homoplasmic m.10197G > A mutation in *MT-ND3* associated with reduced enzyme activity of CI in muscle. Compared with the spectrum of phenotypes seen in 13 previously described families with the same mutation, these children showed some novel clinical features. Two of the boys presented with subacute onset of dystonia, which showed a remitting-relapsing clinical course in one of them. The third boy presented acute symptoms consisting of speech impairment, progressive left-sided hemiparesis, and also vertebral and arterial malformations. In all the children, molecular studies identified a similar mutation load in tissues, and neuroimaging findings were consistent with the features seen in LS. Functional investigations in cultured skin fibroblasts suggested low ATP production in homoplasmic cells. Our results confirm that the m.10197G > A mutation is relevant to these patients' clinical and biochemical phenotypes, which thus expand the array of phenotypes associated with this variant.

1. Introduction

Mitochondrial complex I (NADH ubiquinone oxidoreductase, EC 1.6.5.3, [CI]) catalyzes the oxidation of reduced NADH by CoQ, and it is the largest complex in the mitochondrial respiratory chain (MRC). Seven of its subunits (MT-ND1, ND2, ND3, ND4, ND5, ND6, and ND4L), all part of the catalytic “core” of the holocomplex, are encoded by the mitochondrial genome, whereas the remaining 38 nuclear DNA-encoded subunits are involved in holoenzyme catalysis, assembly, stability and regulation [1]. Isolated CI deficiency is considered the most common genetic defect in MRC disorders, and it is a relatively common etiology in Leigh-like syndrome (LS), accounting for about 30% of cases [2]. Additional, comparatively less frequent, presentations of low CI include mitochondrial encephalomyopathy with lactic acidosis and

Abbreviations: bp, base pairs; CI, complex I; FCCP, carbonyl cyanide 4-(trifluoromethoxy) phenylhydrazone; DAPI, 4′,6-diamidino-2-phenylindole; LHON, Leber hereditary optic neuropathy; LS, Leigh-like syndrome; MELAS, mitochondrial encephalomyopathy with lactic acidosis and stroke-like episodes; MRC, mitochondrial respiratory chain; MRS, MRI spectroscopy; mtDNA, mitochondrial DNA; RFU, relative fluorescence units; OCR, oxygen consumption rate; WB, Western blotting

* Corresponding author at: IRCCS Fondazione Stella Maris, via dei Giacinti 2, 56128, Pisa, Italy.
E-mail addresses: deborah.tolomeo@fsm.unipi.it (D. Tolomeo), mariasavinaseverino@gaslini.org (M. Severino), francesca.pochiero@meyer.it (F. Pochiero), claudiobruno@gaslini.org (C. Bruno), dcassandrini@fsm.unipi.it (D. Cassandrini), annalisamadeo@gaslini.org (A. Madeo), sdoccini@fsm.unipi.it (S. Doccini), marinapedemonte@gaslini.org (M. Pedemonte), andrearossi@gaslini.org (A. Rossi), m.donati@meyer.it (M.A. Donati), majadirocco@gaslini.org (M. Di Rocco), filippo3364@gmail.com, fsantorelli@fsm.unipi.it (F.M. Santorelli).
[1] These authors contributed equally to this work.

https://doi.org/10.1016/j.jns.2019.02.010
Received 16 September 2018; Received in revised form 1 February 2019; Accepted 5 February 2019
Available online 06 February 2019
0022-510X/

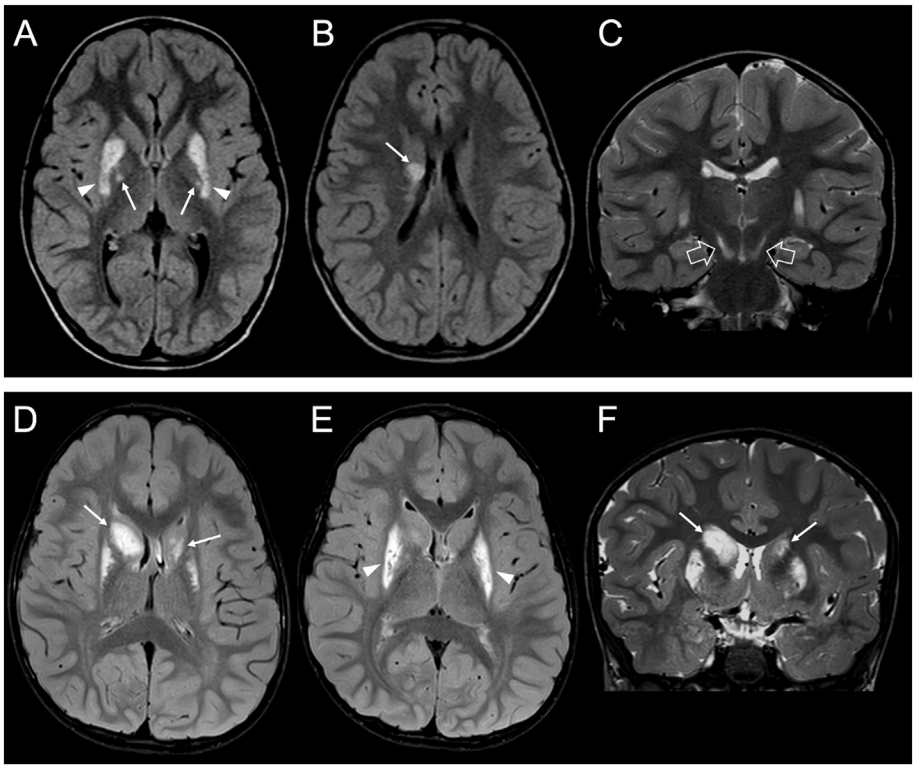

Fig. 1. Brain MRI of patient 1 at 6 years of age (A–C) and patient 3 at 3 years of age (D–F). Patient 1: (A, B) Axial FLAIR images show hyperintense lesions in the putamina (arrowheads) and globi pallidi (thin arrows), and in the right caudate body (arrow). (C) Coronal T2-weighted image depicts involvement of the subthalamic nuclei (empty arrows). Patient 3: (D, E) Axial FLAIR and F) coronal T2-weighted images show bilateral atrophy of the putamen (arrowheads) and acute lesions in the caudate heads (arrows).

stroke-like episodes (MELAS) [3], Leber hereditary optic neuropathy (LHON), and hepatopathy [2,4], cardiomyopathy [5], and syndromic dystonia [6], the latter presenting either in isolation or in various combinations. Respiratory chain CI deficiency shows wide genetic and allelic heterogeneity; most variants occur in the *MT-ND1*, *MT-ND3* and *MT-ND5* genes [2]. Precise descriptions of the clinical and imaging features of specific cohorts harboring the same mutation are scarce [7]. In the present study, previously described cases of the m.10197G > A *MT-ND3* mutation are reviewed and three additional children harboring this gene variant are presented. The phenotypes of these three new cases differ from those of the previously reported ones, and therefore expand the spectrum of features associated with m.10197G > A *MT-ND3*. *In vitro* exploration of the possible impact of the mutation on ATP content and energy production also allowed us to corroborate the disease-causing role of this variant.

2. Materials and methods

2.1. Participants and clinical assessments

The study was performed according to a protocol reviewed and approved by the Tuscany Regional Pediatric Ethics committee. All the procedures complied with the Helsinki Declaration of 1975. Genetic studies were performed after parental written informed consent had been obtained. The three patients we describe are part of a larger group of 130 children with mitochondrial encephalomyopathies of unknown etiology studied in our laboratories. The patients and their available family members were evaluated by five clinicians (M.A.D., M.P., C.B., M.DiR., and F.M.S.).

2.2. Morphological, genetic and biochemical analyses

A diagnostic biopsy of the deltoid muscle was performed in all three children and processed for routine morphology and histochemistry using standard methods. A skin punch biopsy was also performed and fibroblasts were grown in DMEM (Dulbecco's modified Eagle's medium) supplemented with 10% fetal bovine serum, 4.5 g/L glucose and 50 μg/ml uridine. Total genomic DNA was obtained from the probands (extracted from different tissues, *i.e.* muscle, skin fibroblasts and peripheral blood, and from urinary sediment) and from their mothers (blood and urinary sediment), and sequencing of the whole mitochondrial genome from skeletal muscle was performed by massive parallel sequencing using Nextera technology (Illumina, San Diego, CA). An *ad hoc* designed PCR-RFLP strategy was used to quantify the tissue abundance of the mt.10197G > A mutation (see legend to Supplementary Fig. S1). Respiratory chain complex activities in skeletal muscle homogenate were measured using published spectrophotometric methods [8]. Western blotting (WB) analysis was performed using the following antibodies: total OXPHOS Human WB Antibody Cocktail, NDUFA9, and SDHA. Monoclonal anti-GAPDH and β-tubulin were employed as loading controls. All antibodies were from Abcam (Cambridge, UK).

Oxygen consumption rate (OCR) was measured in adherent fibroblasts with an XFe24 Extracellular Flux Analyzer (Seahorse Bioscience, Agilent, Santa Clara, CA). Cells were seeded at a density of 50×10^3 cells/well and incubated for 24 h at 37 °C before starting the assay procedure. Measurements of endogenous respiration were performed with a non-buffered medium. After baseline recording, OCR was measured after sequentially adding oligomycin, carbonyl cyanide 4-(trifluoromethoxy) phenylhydrazone (FCCP) and Rotenone/antimycin A to reach working concentrations of 2 μM, 2 μM and 0.5/0.5 μM, respectively. Post-assay plates were washed in PBS and fixed/permeabilized in 4% PFA/0.1% Triton X-100 following 4′,6-diamidino-2-phenylindole (DAPI) staining for 10 min at room temperature. Fluorescence, as a function of number of cells, was measured for each well at 358/461 nm Ex/Em using a SpectraMax iD3 Multi-Mode Microplate Reader (Molecular Devices LLC, San Jose, CA). Prior to data analysis, fluorescence data were transferred to Seahorse Wave 2.4 Software (Agilent) for OCR normalization performed using a Seahorse Bioscience Report Generator. Data were expressed as pmol O_2/min/relative fluorescence units (RFU) and presented as the average of seven replicate wells ± SD.

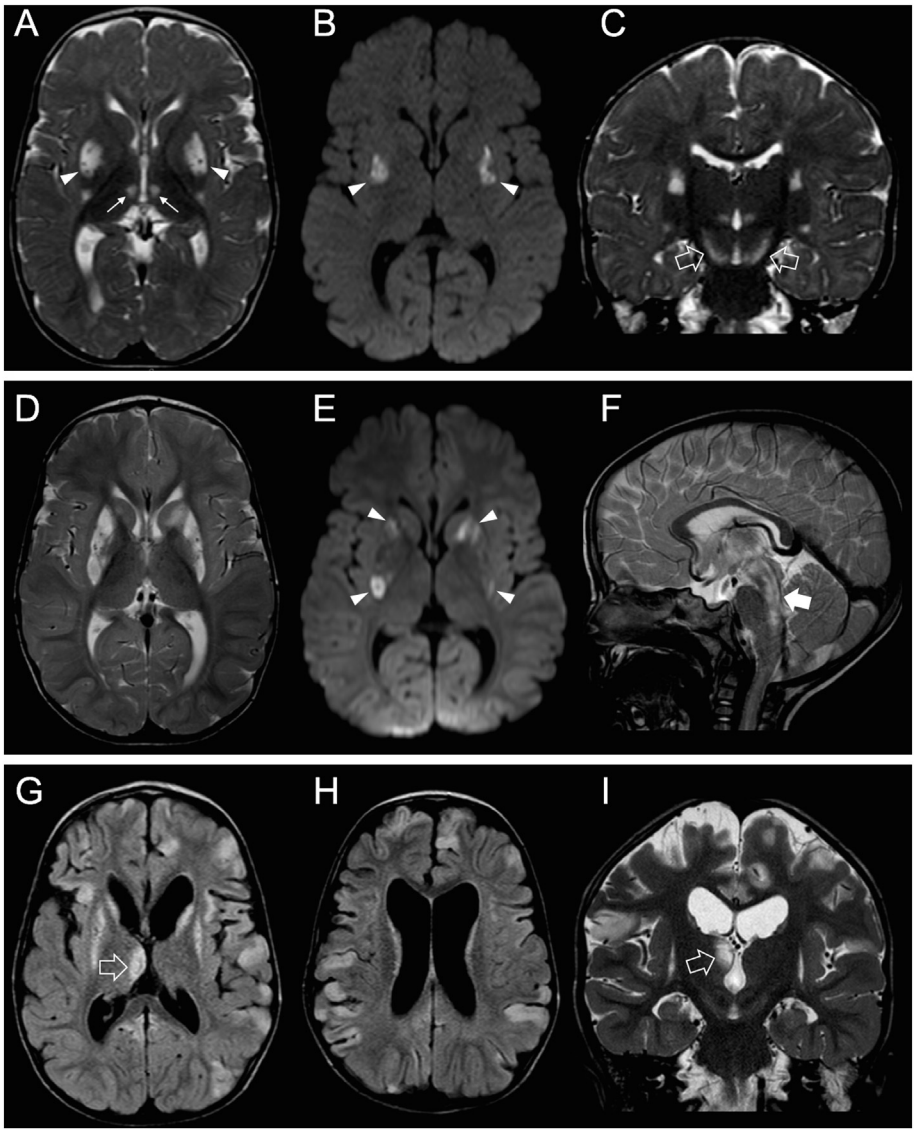

Fig. 2. Brain MRI of patient 2 performed at 9 months (A–C), 17 months (D–F) and 5 years of age (G–I). (A) Axial T2-weighted image reveals bilateral symmetrical T2 signal abnormalities at the level of the putamina (arrowheads) and mesial portion of the thalami (thin arrows). (B) Corresponding diffusion-weighted image demonstrates restricted diffusion in the intermediate portion of the putamina (arrowheads). (C) Coronal T2-weighted image shows additional involvement of the subthalamic nuclei (empty arrows). Axial T2-weighted (D) and diffusion-weighted (E) images at 17 months of age reveal new bilateral lesions with restricted diffusion in the putamen and caudate nuclei (arrowheads). (F) Sagittal T2-weighted image shows severe dorsal brainstem involvement (thick arrow). (G, H) Axial FLAIR and (I) coronal T2-weighted images performed at 5 years of age demonstrate basal ganglia atrophy and new hyperintense multifocal lesions in the right medial thalamus (empty arrows) and cortico-subcortical regions. The white matter volume is reduced due to secondary ventricular dilatation and enlarged subarachnoid spaces.

3. Results

3.1. Case reports

The first patient (Pt1) was a 7-year-old boy, the third child of healthy unrelated parents. His prenatal and perinatal periods were reported to be unremarkable and his psychomotor development was normal. The family history was negative both for neurological disorders and visual impairment. At the age of 6 years, the child suddenly began to display abnormal gait and right lower limb dystonia and stiffness, followed by rigidity of the right upper limb with hand dystonia. Brain MRI showed bilateral T2 and FLAIR hyperintensity of the putamina, subthalamic nuclei and substantia nigra, associated with focal restricted diffusion in the right caudate body. The globus pallidus was partially involved, bilaterally (Fig. 1A–C). Routine blood tests including plasma copper, ceruloplasmin, amino acids, urine organic acids, serum lactate, lactate/pyruvate ratio, as well as cerebrospinal fluid analyses were all normal. The lactate was not tested in the CSF. Neurophysiological investigations and video-EEG recording showed no abnormalities. Over the following few months, there was a partial, spontaneous motor recovery leaving the child with mild dystonic postures and moderate rigidity of the lower limb. At the age of 7 years, the child experienced another spontaneous subacute episode of left lower limb dystonia. There were no identifiable premonitory symptoms or triggers of the sudden neurological deficit. Brain MRI showed bilateral putamen volume loss, persistent T2 hyperintensity of the right caudate body, and a new lesion in the left caudate head (data not shown).

The second child (Pt2) was a 5-year-old boy with an unremarkable family history. He had displayed moderate perinatal respiratory distress. He presented dysmorphic features, horseshoe kidneys, mid-aortic syndrome, scoliosis due to vertebral malformations (Supplementary Fig. S2), and a systolic cardiac murmur, as well as diffuse hypotonia with limb dystonia, muscle strength reduction and atrophy. He was able to walk only with bilateral support. Blood tests revealed increased lactate levels (9.97 nM/L, normal < 2). The pyruvic acid levels were not measured. The lactate was not tested in the CSF. Brain MRI performed at 9 months of age had demonstrated bilateral symmetrical T2 signal abnormalities with restricted diffusion at the level of the subthalamic nuclei, putamen and mesial portion of the thalami (Fig. 2A–C). Follow-up MRI study performed at 17 months revealed new brainstem lesions, with prevalent involvement of the pontine tegmentum, midbrain nuclei and basal ganglia (Fig. 2D). At 5 years of age neuroimaging showed symmetrical basal ganglia atrophy and bilateral multifocal cortico-subcortical stroke-like lesions, especially in the frontal, parietal and insular regions, characterized by prevalent subcortical vasogenic edema and small areas of cortical cytotoxic edema (Fig. 2G–I). MRI

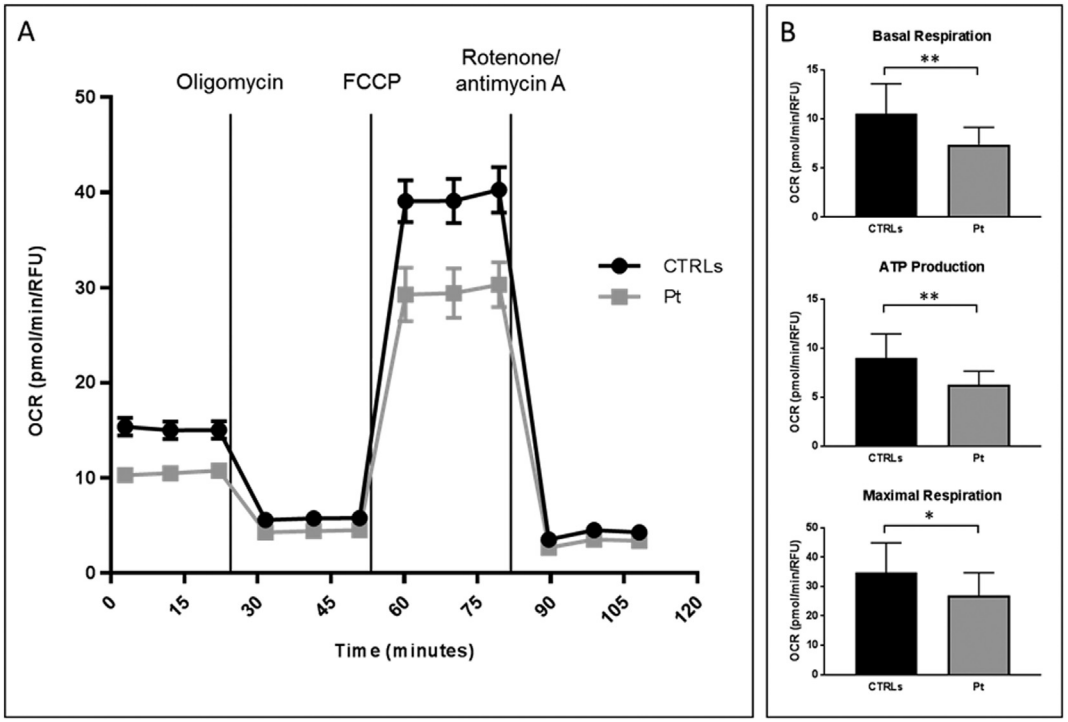

Fig. 3. Microrespirometry in skin fibroblasts from patient 3. Basal respiration indicates the energetic demand of the cell under baseline conditions. The decrease in oxygen consumption rate (OCR) upon injection of the ATP synthase inhibitor oligomycin represents the portion of basal respiration used to drive ATP production. The maximal oxygen consumption rate attained by adding the uncoupler FCCP, mimicking a physiological "energy demand", indicates the maximum rate of respiration that the cell can achieve. The fraction of non-mitochondrial oxygen consumption is measured after complete inhibition of the mitochondrial respiratory chain by a mix of antimycin A and rotenone. (A) Kinetic microscale oxygraphy graphs depicting OCR means ± SEM generated using the Seahorse Biosciences extracellular flux analyzer. (B) Metabolic parameters obtained from OCR profiling and reported as means and SD in histograms. Data refer to three independent experiments. CTRLs: cells from healthy controls; Pt: cells from patient 3. Statistical significance was calculated using an unpaired *t*-test to compare controls and patient group. $^{**}p < .01$; $^{*}p < .05$.

spectroscopy (MRS) studies performed at the level of right basal nuclei thalamus showed inverted lactate peaks with normal *N*-acetyl aspartate, while at the level of left temporal cortex revealed more pronounced inverted lactate peaks associated with reduction of *N*-acetyl aspartate (Supplementary Fig. S3). Arterial magnetic resonance angiography was normal. This overall pattern was suggestive of a MELAS/LS overlap syndrome with progressive cortical lesions and brain atrophy. Subsequently, he presented episodes of absence, generalized tonic and tonic-clonic seizures and the last EEG, performed at the age of eight years, showed clear bilateral epileptiform anomalies on fronto-temporal areas with tendency to spread to both sides. He is currently taking anticonvulsant medications (Levitiracetam, Lamotrigine, and Clobazam) but he is not receiving specific therapy for dystonia.

The third child (Pt3), a 4-year-old boy, was born at term to non-consanguineous and healthy parents. He had normal prenatal and perinatal medical histories. His psychomotor development was unremarkable until the age of 16 months when he experienced a severe episode of bronchopneumonia, which was followed by slight motor regression. At 31 months, his parents requested an in-depth evaluation because of frequent falls and gait difficulty. At the age of 3 years, the boy began to display progressive left-sided hemiparesis; this was accompanied by a worsening of gait, together with postural instability and muscle weakness. Subsequently, he developed a speech disorder (stuttering and slurred speech). Routine blood tests were uninformative. CSF analysis was within normal limits, CSF lactate not tested. Brain MRI showed bilateral T2 hyperintense lesions of the putamina, caudate heads and dentate nuclei (Fig. 1D–F). Magnetic resonance angiography was uninformative. MRS showed a lactate peak in normal-appearing right fronto-parietal cortex and subcortical white matter (Supplementary Fig. S4).

There were no reports of apparent cognitive deterioration, loss of vision or ophthalmoplegia in any of the three patients.

3.2. Laboratory investigations

Histochemical analysis of muscle biopsy samples was uninformative in Pt1, revealed slightly reduced oxidative metabolism in Pt2, and showed mild lipid accumulation with subsarcolemmal mitochondrial proliferation in Pt3 (not shown). Spectrophotometric determination of MRC complex activities in muscle and WB both showed a slight and isolated deficiency of CI in all cases (residual activity was 72%, 78% and 54% normal in Pt1, Pt2 and Pt3, respectively). In all the patients, whole mtDNA direct sequencing identified the m.10197G > A/p.Ala47Thr mutation in the *MT-ND3* subunit of CI. *Ad hoc* designed PCR-RFLP analyses revealed virtually homoplasmic mutation levels in blood, muscle, skin fibroblasts and urinary sediment in Pt1 (data not shown) and Pt2, whereas Pt3 showed a mutation load of > 95%. The mother of Pt1 repeatedly refused genetic testing, while the asymptomatic mother of Pt2 harbored nearly absent mutant mitochondrial genomes, and Pt3's mother presented extremely low levels of mutant genomes in blood and a mutation load of 6.8% in urinary sediment (Supplementary Fig. S1). No additional maternal relatives could be examined. Using microscale oxygraphy to evaluate the impact of the mutation on mitochondrial respiration, in patient 3's fibroblasts we observed significantly reduced basal and maximal respiratory capacities, together with a low mitochondrial ATP output (Fig. 3A–B). Similar results were seen in the other two children (data not shown).

4. Discussion

Mutations in mtDNA in children result in highly variable clinical phenotypes including, among others, LS, lethal infantile mitochondrial

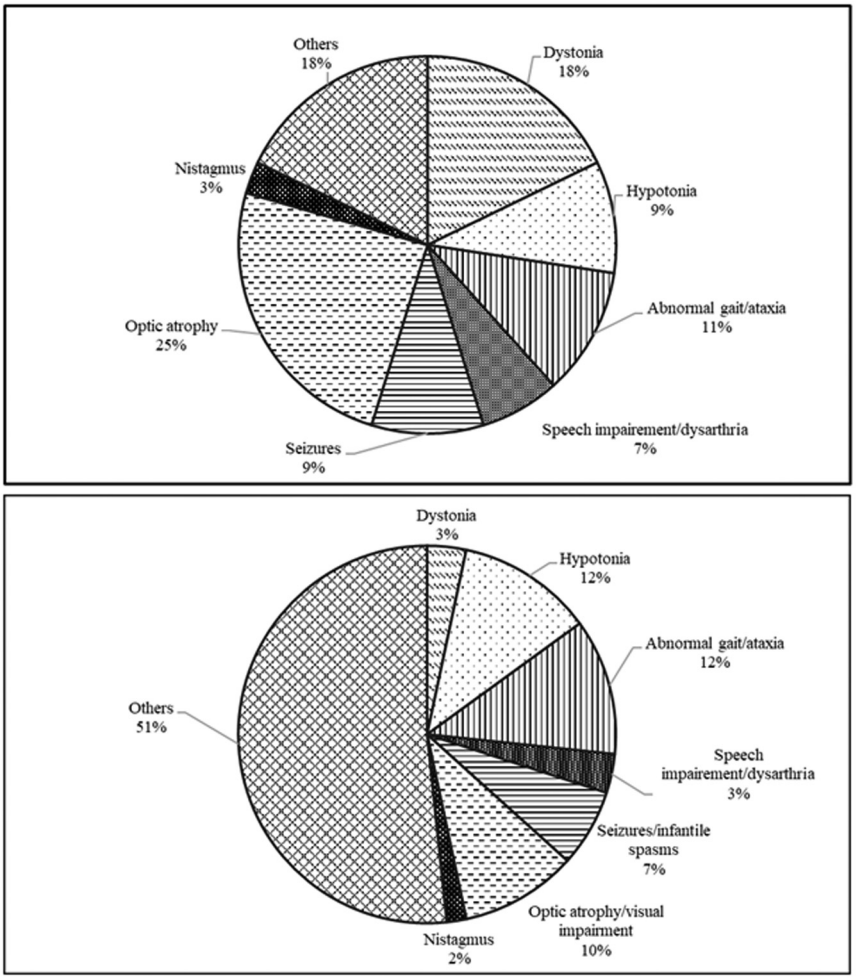

Fig. 4. Literature review of main clinical presentations associated with the *MT-ND3* m.10197G > A. Data were compared with those detected in the relatively more common m.13513 G > A mutation in *MT-ND5*. (A) Frequency of clinical features associated with the *MT-ND3* m.10197G > A mutation expressed as percentages. *Others: neuromuscular involvement, strabismus, growth retardation, anorexia, emotional lability, psychomotor regression and hearing loss. (B) Frequency of *MT-ND5* m.13513 G > A-associated clinical presentations expressed as percentages. *Others: neuromuscular involvement, strabismus, respiratory disturbance, gastrointestinal dysmotility, Wolff-Parkinson-White syndrome, cardiomyopathy, emotional lability, psychomotor regression, retinal dystrophy and hearing loss.

disease (fatal congenital lactic acidosis), isolated cardiomyopathy, isolated hepatopathy, and MELAS syndrome [9]. However, genotype and clinical manifestations remain poorly correlated in this setting. Several variants clustered in CI genes recur in unrelated families with isolated biochemical deficiencies, but descriptions of the full sets of associated clinical and imaging phenotypes tend to be scarce, although there are a few exceptions (*e.g.*, m.13513G > A in *MT-ND5*, m.10191T > C in *MT-ND3*, the common LHON mutation m.11778G > A in *MT-ND4*). In other cases, such as the m.10197G > A mutation in *MT-ND3* identified in the patients here reported, mutations are judged to be disease related or not solely on the basis of *in silico* criteria or their high frequency in specific populations or haplogroups [10–13]. In these cases, *in vitro* or *in vivo* functional evidence is needed to establish the true pathogenic significance of the mutations.

The present investigation of three new children presenting the m.10197G > A mutation in *MT-ND3* allows us to confirm the close link between abundant mutant mitochondrial genomes and impaired basal and maximal respiratory capacity in tissues showing low CI activity. Although none of the patients' mothers seemed to harbor the mutation at significant levels, it should be noted that an apparent *de novo* origin of the m.10197G > A mutation has previously been described [9]. Combining the microscale oxygraphy results with those of biochemical studies in muscle, we observed that almost homoplasmic mutant mtDNA levels impair CI activity and reduce maximal respiration by 30% (Fig. 3B). These data are in keeping with the location of the m.10197G > A mutation at a protein region critical for conformational changes occurring during CI catalytic turnover [14].

In the present study, as well as adding new biochemical information on this particular mtDNA variant, we also expanded the spectrum of clinical features associated with it, adding impaired speech, relapsing-remitting episodes of focal dystonia and stroke-like episodes (the latter reported, to date, in a single work [15]) to the previously described array of clinical presentations. Reviewing published data on patients harboring the m.10197G > A mutation [2,10,15–20] we observed that clinical data, when available, mainly consisted of stable dystonia (38% of patients) associated (in 31% of these cases) with hypotonia or gait ataxia, and less commonly, seizures (20% of patients), dysarthria (15% of patients), or variable neuromuscular involvement (Fig. 4; Supplementary Table S1). In a single large family, Leber dystonia was observed [17]. Neuroimaging findings, when available, were suggestive of LS or MELAS/LS overlap syndrome, as in our cases. The relatively high frequency of dystonic postures at onset or early in the disease course, as seen in two of our patients, and remitting-relapsing course, as seen in one of them, seem to distinguish this variant from other mtDNA-associated CI deficiency changes, regardless of the relatively unspecific neuroimaging data. Indeed, highly similar MRI features have been described in patients harboring the m.13513G > A mutation in *MT-ND5* [7], in whom sudden onset of dystonia has never been reported. In the era of precision medicine, our data, identifying sudden-onset and relapsing movement disorders as highly specific features of the m.10197G > A variant, could facilitate new diagnoses in children with similar manifestations.

The acute, at times remitting-relapsing, clinical course was documented in our cases by follow-up brain imaging, but the precise mechanism underlying these features remains unclear. We are tempted to speculate that the high levels of the mutation we measured in peripheral tissues were equally high in the basal ganglia, and impeded the functional and structural stability of mutated mitochondria in the

putamen. Whether this leads to a transient decrease in energy demands locally, and correlates with relapses of clinical manifestations remains to be demonstrated, but a similar process is thought to occur in the context of LS, both during seizures and/or in the presence of high fever. Importantly, some degree of metabolic energy impairment and mitochondrial dysfunction is also found in other rare movement disorders characterized by sudden attacks of involuntary movements [21].

A final observation can be drawn from the sudden-onset motor impairment seen in Pt2. This child had manifestations mimicking MELAS associated with LS-like brain MRI, a combination already described in children carrying the m.13513G > A mutation in *MT-ND5* [15,22–24]. These features are likely the consequence of "metabolic" strokes, characterized on MRI by slowly progressive spread of cortico-subcortical lesions with mixed cytotoxic and vasogenic edema, crossing vascular boundaries and evolving in regional brain atrophy with normal intracranial arteries [25,26] The same patient showed several extracranial malformative features, including renal and vertebral anomalies consistent with a VACTERL-like phenotype (see Supplementary Fig. S2). Of note, congenital anomalies have been described in several patients with mitochondrial disorders, but are likely under-recognized and underreported [27,28]. The underlying mechanism is not well understood, although it has been hypothesized that the abnormal embryonal development might be the result of reduced energy supply that could affect the rate of cell divisions [29].

To summarize, the m.10197G > A mutation appears to be a relatively common mitochondrial mutation associated with low ATP output and basal ganglia involvement on neuroimaging. Sudden onset of dystonic postures in young children or teens with LS-/MELAS-like MRI features should lead the clinicians caring for them to consider this mutation.

Supplementary data to this article can be found online at https://doi.org/10.1016/j.jns.2019.02.010.

Acknowledgements

This work was partially supported by grants MITO-NEXT Conto capitale (to FMS) and Ricerca Corrente 5x1000 2016–2017 (to CN) from the Italian Ministry of Health.

We thank Dr. Catherine J. Wrenn for expert editing of the manuscript and critical advice on tables and figures.

Authors' disclosure

Tolomeo Deborah: reports no disclosures.
Rubegni Anna: reports no disclosures.
Severino Mariasavina: reports no disclosures.
Pochiero Francesca: reports no disclosures.
Bruno Claudio: reports no disclosures.
Cassandrini Denise: reports no disclosures.
Madeo Annalisa: reports no disclosures.
Doccini Stefano: reports no disclosures.
Pedemonte Marina: reports no disclosures.
Rossi Andrea: reports no disclosures.
D'Amore Francesca: reports no disclosures.
Donati M. Alice: reports no disclosures.
Di Rocco Maja: reports no disclosures.
Santorelli Filippo M: reports no disclosures.
Nesti Claudia: reports no disclosures.

References

[1] W.J.H. Koopman, L.G.J. Nijtmans, C.E.J. Dieteren, P. Roestenberg, F. Valsecchi, J.A.M. Smeitink, P.H.G.M. Willems, Mammalian mitochondrial complex I: biogenesis, regulation, and reactive oxygen species generation, Antioxid. Redox Signal. 12 (2010) 1431–1470, https://doi.org/10.1089/ars.2009.2743.

[2] H. Swalwell, D.M. Kirby, E.L. Blakely, A. Mitchell, R. Salemi, C. Sugiana, A.G. Compton, E.J. Tucker, B.-X. Ke, P.J. Lamont, D.M. Turnbull, R. McFarland, R.W. Taylor, D.R. Thorburn, Respiratory chain complex I deficiency caused by mitochondrial DNA mutations, Eur. J. Hum. Genet. 19 (2011) 769–775, https://doi.org/10.1038/ejhg.2011.18.

[3] R. Horváth, R. Reilmann, E. Holinski-Feder, E.B. Ringelstein, T. Klopstock, The role of complex I genes in MELAS: a novel heteroplasmic mutation 3380G > A in ND1 of mtDNA, Neuromuscul. Disord. 18 (2008) 553–556, https://doi.org/10.1016/J.NMD.2008.05.002.

[4] E. Fassone, S. Rahman, Complex I deficiency: clinical features, biochemistry and molecular genetics, J. Med. Genet. 49 (2012) 578–590, https://doi.org/10.1136/jmedgenet-2012-101159.

[5] E. Fassone, J.W. Taanman, I.P. Hargreaves, N.J. Sebire, M.A. Cleary, M. Burch, S. Rahman, Mutations in the mitochondrial complex I assembly factor NDUFAF1 cause fatal infantile hypertrophic cardiomyopathy, J. Med. Genet. 48 (2011) 691–697, https://doi.org/10.1136/jmedgenet-2011-100340.

[6] R. Benecke, P. Strümper, H. Weiss, Electron transfer complex I defect in idiopathic dystonia, Ann. Neurol. 32 (1992) 683–686, https://doi.org/10.1002/ana.410320512.

[7] K. Sonam, P.S. Bindu, A.B. Taly, C. Govindaraju, N. Gayathri, H.R. Arvinda, M. Nagappa, S. Sinha, N.A. Khan, P. Govindaraj, K. Thangaraj, Clinical and neuroimaging features in two children with mutations in the mitochondrial ND5 gene, Neuropediatrics 46 (2015) 277–281, https://doi.org/10.1055/s-0035-1550149.

[8] C. Nesti, M.C. Meschini, B. Meunier, M. Sacchini, S. Doccini, A. Romano, S. Petrillo, I. Pezzini, N. Seddiki, A. Rubegni, F. Piemonte, M.A. Donati, G. Brasseur, F.M. Santorelli, Additive effect of nuclear and mitochondrial mutations in a patient with mitochondrial encephalomyopathy, Hum. Mol. Genet. 24 (2015) 3248–3256, https://doi.org/10.1093/hmg/ddv078.

[9] V. Nesbitt, P.J. Morrison, E. Crushell, D.E. Donnelly, C.L. Alston, L. He, R. McFarland, R.W. Taylor, The clinical spectrum of the m.10191T > C mutation in complex I-deficient Leigh syndrome, Dev. Med. Child Neurol. 54 (2012) 500–506, https://doi.org/10.1111/j.1469-8749.2012.04224.x.

[10] D.M. Kirby, R. Salemi, C. Sugiana, A. Ohtake, L. Parry, K.M. Bell, E.P. Kirk, A. Boneh, R.W. Taylor, H.-H.M. Dahl, M.T. Ryan, D.R. Thorburn, NDUFS6 mutations are a novel cause of lethal neonatal mitochondrial complex I deficiency, J. Clin. Invest. 114 (2004) 837–845, https://doi.org/10.1172/JCI20683.

[11] M. Ingman, H. Kaessmann, S. Pääbo, U. Gyllensten, Mitochondrial genome variation and the origin of modern humans, Nature 408 (2000) 708–713, https://doi.org/10.1038/35047064.

[12] D. Mishmar, E. Ruiz-Pesini, P. Golik, V. Macaulay, A.G. Clark, S. Hosseini, M. Brandon, K. Easley, E. Chen, M.D. Brown, R.I. Sukernik, A. Olckers, D.C. Wallace, Natural selection shaped regional mtDNA variation in humans, Proc. Natl. Acad. Sci. U. S. A. 100 (2003) 171–176, https://doi.org/10.1073/pnas.0136972100.

[13] H.-J. Bandelt, A. Salas, R.W. Taylor, Y.-G. Yao, Exaggerated status of "novel" and "pathogenic" mtDNA sequence variants due to inadequate database searches, Hum. Mutat. 30 (2009) 191–196, https://doi.org/10.1002/humu.20846.

[14] A. Galkin, B. Meyer, I. Wittig, M. Karas, H. Schägger, A. Vinogradov, U. Brandt, Identification of the mitochondrial ND3 subunit as a structural component involved in the active/deactive enzyme transition of respiratory complex I, J. Biol. Chem. 283 (2008) 20907–20913, https://doi.org/10.1074/jbc.M803190200.

[15] Y. Leng, Y. Liu, X. Fang, Y. Li, L. Yu, Y. Yuan, Z. Wang, The mitochondrial DNA 10197 G > A mutation causes MELAS/Leigh overlap syndrome presenting with acute auditory agnosia, Mitochondrial DNA 26 (2015) 208–212, https://doi.org/10.3109/19401736.2014.905860.

[16] E. Sarzi, M.D. Brown, S. Lebon, D. Chretien, A. Munnich, A. Rotig, V. Procaccio, A novel recurrent mitochondrial DNA mutation in ND3 gene is associated with isolated complex I deficiency causing Leigh syndrome and dystonia, Am. J. Med. Genet. A 143A (2007) 33–41, https://doi.org/10.1002/ajmg.a.31565.

[17] K. Wang, Y. Takahashi, Z.-L. Gao, G.-X. Wang, X.-W. Chen, J. Goto, J.-N. Lou, S. Tsuji, Mitochondrial ND3 as the novel causative gene for Leber hereditary optic neuropathy and dystonia, Neurogenetics 10 (2009) 337–345, https://doi.org/10.1007/s10048-009-0194-0.

[18] L. Valente, D. Piga, E. Lamantea, F. Carrara, G. Uziel, P. Cudia, A. Zani, L. Farina, L. Morandi, M. Mora, A. Spinazzola, M. Zeviani, V. Tiranti, Identification of novel mutations in five patients with mitochondrial encephalomyopathy, Biochim. Biophys. Acta Bioenerg. 1787 (2009) 491–501, https://doi.org/10.1016/j.bbabio.2008.10.001.

[19] S.E. Calvo, V.K. Mootha, The mitochondrial proteome and human disease, Annu. Rev. Genomics Hum. Genet. 11 (2010) 25–44, https://doi.org/10.1146/annurev-genom-082509-141720.

[20] Z. Chen, Z. Zhao, Q. Ye, Y. Chen, X. Pan, B. Sun, H. Huang, A. Zheng, et al., Mol. Med. Rep. 11 (2015) 1956–1962, https://doi.org/10.3892/mmr.2014.2911.

[21] D. Ghezzi, C. Canavese, G. Kovacevic, D. Zamurovic, C. Barzaghi, C. Giorgi, G. Zorzi, M. Zeviani, P. Pinton, B. Garavaglia, N. Nardocci, A family with paroxysmal nonkinesigenic dyskinesias (PNKD): evidence of mitochondrial dysfunction, Eur. J. Paediatr. Neurol. 19 (2015) 64–68, https://doi.org/10.1016/j.ejpn.2014.10.003.

[22] M.J. Blok, L. Spruijt, F.M. De, Mutations in the ND5 subunit of complex I of the mitochondrial DNA are a frequent cause of oxidative phosphorylation disease, J. Med. Genet. 44 (2007) 74, , https://doi.org/10.1136/jmg.2006.045716.

[23] Z. Wang, X.K. Qi, S. Yao, B. Chen, X. Luan, W. Zhang, M. Han, Y. Yuan, Phenotypic patterns of MELAS/LS overlap syndrome associated with m.13513G > A mutation, and neuropathological findings in one autopsy case, Neuropathology 30 (2010) 606–614, https://doi.org/10.1111/j.1440-1789.2010.01115.x.

[24] C.D.M. Van Karnebeek, P.J. Waters, M.A. Sargent, M.M. Mezey, L.-J. Wong, J. Wang, S. Stöckler-Ipsiroglu, S. Stöckler-Ipsiroglu, Expanding the clinical phenotype of the mitochondrial m.13513G > A mutation with the first report of a fatal

neonatal presentation, Dev. Med. Child Neurol. 53 (2011) 565–568, https://doi.org/10.1111/j.1469-8749.2010.03907.x.
[25] C.L. Alston, M.C. Rocha, N.Z. Lax, D.M. Turnbull, R.W. Taylor, The genetics and pathology of mitochondrial disease, J. Pathol. 241 (2017) 236–250, https://doi.org/10.1002/path.4809.
[26] Y.S. Ng, N.Z. Lax, P. Maddison, C.L. Alston, E.L. Blakely, P.D. Hepplewhite, G. Riordan, S. Meldau, P.F. Chinnery, G. Pierre, E. Chronopoulou, A. Du, I. Hughes, A.A. Morris, S. Kamakari, G. Chrousos, R.J. Rodenburg, C.G.J. Saris, C. Feeney, S.A. Hardy, T. Sakakibara, A. Sudo, Y. Okazaki, K. Murayama, H. Mundy, M.G. Hanna, A. Ohtake, A.M. Schaefer, M.P. Champion, D.M. Turnbull, R.W. Taylor, R.D.S. Pitceathly, R. McFarland, G.S. Gorman, MT-ND5 mutation exhibits highly variable neurological manifestations at low mutant load, EBioMedicine 30 (2018) 86–93, https://doi.org/10.1016/J.EBIOM.2018.02.010.
[27] S. Siebel, B.D. Solomon, Mitochondrial factors and VACTERL association-related congenital malformations, Mol. Syndromol. 4 (2013) 63–73, https://doi.org/10.1159/000346301.
[28] M. Thomas, V. Salpietro, N. Canham, M. Ruggieri, R. Phadke, M. Kinali, Mitochondria DNA depletion syndrome in a infant with multiple congenital malformations, severe myopathy, and prolonged postoperative paralysis, J. Child Neurol. 30 (2015) 654–658, https://doi.org/10.1177/0883073814532546.
[29] M. Lubinsky, Embryonic hypocellularity, blastogenetic malformations, and fetal growth restriction, Am. J. Med. Genet. A 173 (2017) 151–156, https://doi.org/10.1002/ajmg.a.37985.